Applied Catalysis B: Environmental 172–173 (2015) 82–90

Contents lists available at ScienceDirect

Applied Catalysis B: Environmental

journal homepage: www.elsevier.com/locate/apcatb

Importance of electrode hot-pressing conditions for the catalyst performance of proton exchange membrane fuel cells

Shuang Ma Andersen [a,*], Rajnish Dhiman [a], Mikkel Juul Larsen [b], Eivind Skou [a]

[a] Department of Chemical Engineering, Biotechnology and Environmental Technology, University of Southern Denmark, Niels Bohrs Allé 1, DK-5230 Odense M, Denmark
[b] IRD Fuel Cells A/S, Kullinggade 31, DK-5700 Svendborg, Denmark

ARTICLE INFO

Article history:
Received 2 January 2015
Received in revised form 13 February 2015
Accepted 20 February 2015
Available online 21 February 2015

Keywords:
PEMFC
Interface
Hot-pressing
Ionomer
Durability

ABSTRACT

The catalyst performance in a proton exchange membrane fuel cell (PEMFC) depends on not only the choice of materials, but also on the electrode structure and in particular on the interface between the components. In this work, we demonstrate that the hot-pressing conditions used during electrode lamination have a great influence on the catalyst properties of a low-temperature PEMFC, especially on its durability. Lamination pressure, temperature and duration were systematically studied in relation to the electrochemical surface area, platinum dissolution, platinum particle size and electrode surface composition. The degradation of the platinum catalyst and polymer was analyzed in relation to the preparation conditions. An optimal electrode interface structure can improve Pt performance by (1) providing high platinum utilization; (2) decreasing platinum migration and coalescence; (3) reducing carbon corrosion triggered platinum detachment; and (4) influencing transport property of the soluble platinum species (SPS) which may redeposit. Strict control of the lamination conditions is needed in order to avoid damage of the polymer and degradation of the catalyst.

1. Introduction

After nearly five decades of fundamental and technological developments, the proton exchange membrane fuel cells (PEMFCs) are getting closer to the market than ever before. However, durability is still an issue. More robust and stable fuel cell materials [1,2] are vital to reach this goal. Moreover, good understanding of the degradation mechanisms [3–5] is also crucial for the general development strategy. Among various operation conditions, load changing and start/stop cycles can lead to almost 90% of the PEM fuel cell performance degradation [6] and a fuel cell in a vehicle may have a lifetime of only one tenth of the one in a stationary power supply [7,8]. Thus, manipulation of potential or current in connection with accelerated stress test on the fuel cell related components has been a focus of the research.

Instability of the platinum electrocatalyst is one of the important causes of degradation in PEMFCs. Though it is still not fully understood, platinum nanoparticle degradation mechanisms [9] in a typical hydrogen fuel cell can be generally categorized into: (1) Ostwald ripening: dissolved Pt species from smaller particles redeposit onto the surfaces of larger particles; (2) Pt migration and coalescence: Pt nanoparticles migrate on the surface of a carbon support and coalesce; (3) Pt detachment and agglomeration: Pt nanoparticles detach from the carbon support and/or agglomerate due to the carbon corrosion and (4) Pt reduction in the polymer: Pt ions are reduced and precipitated out in the polymer phase by chemical reduction by hydrogen.

Modification of the catalyst-support interaction [10,11] is one of the effective methods to enhance the catalyst activity and durability as observed in various fundamental materials research. Electron sharing between orbitals of the catalyst and the support or Pt binding energy shift to higher energy level provides platinum better stability and higher resistance to oxidation. However, other approaches within electrode structure and interface, especially involving proton conducting phase, were not sufficiently explored.

Kulikovsky [12] studied accelerated stress tests (ASTs) published by three groups, focusing on potential cycling, open-cell voltage holding and humidity cycling, respectively, by fitting analysis. It was shown that the major failure modes of the PEMFCs are a dramatic lowering of oxygen diffusivity and proton conductivity at the cathode catalyst layer; while, there was only a minor decrease of the catalyst mass activity. This indicates that the catalyst degradation may not be the bottleneck, but that low mass and proton transports are rather the barriers of the processes. Therefore, the

* Corresponding author. Tel.: +45 6550 9186.
E-mail address: mashu@kbm.sdu.dk (S.M. Andersen).

http://dx.doi.org/10.1016/j.apcatb.2015.02.023
0926-3373/

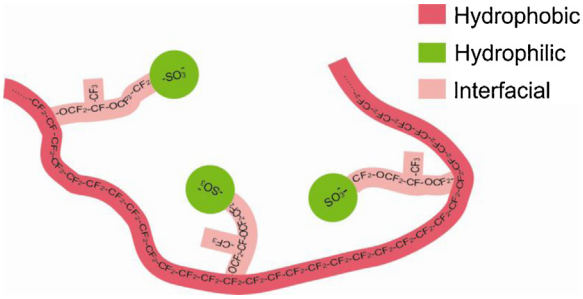

Fig. 1. Chemical structure of Nafion.

Table 1
Sample list with the corresponding hot-pressing conditions

Electrode	ID	Pressure/bar	Temperature/°C	Duration/min
Non-laminated	CIE0	0	25	0
Laminated	CIE1	3	150	3
	CIE2	5	150	3
	CIE3	7	150	3
	CIE4	7	100	3
	CIE3	7	150	3
	CIE5	7	200	3
	CIE6	7	150	1
	CIE3	7	150	3
	CIE7	7	150	

stability of the catalyst region, where it has simultaneous access to the electron, proton and mass phases (or the so called three-phase boundary – TPB), is a key to the issue. A detailed understanding of the interface structure and the associated degradation mechanism will certainly assist in overcoming the challenges in the current fuel cell technology.

Various proton conducting polymers, such as non-fluorinated polyaryl (sulfonated polyether (ether) ketone, SPEEK), polystyrene sulfonic acid (PSSA) and perfluorosulfonic acid (PFSA), have been tested as electrolyte in PEMFCs. To date, PFSA is the most widely studied and applied proton conducting polymer in PEMFCs. PFSAs are a group of comb-shaped macro molecules with a fluorocarbon backbone and sulfonated perfluoroalkyl ether side chains. Fig. 1 illustrates the chemical structure of the most commonly used low-temperature PEMFC ionomer, Nafion®.

Due to its exclusive chemical structure and self-organizing ability, Nafion provides many advantages as a catalyst layer component. The typical loading of the ionomer in a PEMFC electrode is between 30 and 50% by weight [13,14], depending on the surface properties of the catalyst and the support. Since the density [15] of Nafion is around 1.5 g/cm^3, a composite electrode normally contains 40–60% ionomer by volume, depending also on hydration. This suggests that the final interface structure of the electrode has a significant contribution from the polymer phase. The interaction between the catalyst and the proton conductor is thus one of the most important factors affecting the three-phase boundary.

The electrode performance and durability is greatly related to the interface structure, which can be affected through many parameters, such as choice of electrode components (their associated hydrophobicity) [16], ink additives [17], electrode preparation [18] MEA fabrication [19,20] etc. Here we focus on the electrode properties affected by the hot-pressing conditions.

As the only appropriate joining technology for PEMFCs, hot-pressing (or lamination, welding) promotes coalescence of the bonding partners by applying pressure and heat to the interface. Due to the heterogeneous nature of the catalyst layer, the adhesion at the interface of two jointed parts can be explained by a variety of possible adhesion models [21,22] such as the thermodynamic adhesion, the chemical adhesion, the electrical adhesion, the diffusion adhesion and the most classical model of the mechanical adhesion.

The mechanical [23,24] (Young's modulus, toughness, fracture, creep, relaxation rates, etc.) and physiochemical [25] (water uptake, conductivity, crystallinity, glass transition temperature, etc.) properties of Nafion have been extensively studied in the past years. Moreover, the mechanical properties of hot pressed membrane were recently reported [26]. It demonstrated that the adhesion force between two pieces of membrane was affected by temperature, pressure and process time, which are common fabrication conditions applied to the electrode. In a PEMFC, close connection between the electrodes and the membrane is important for the proton transport from the anode to the cathode. Moreover, intimate contact between the ionomers and the catalysts in the electrodes, and an associated robust ionomer network in the catalyst layers, are even more critical for the electrochemical reactions. Recently, the electrode fabrication conditions were also studied from an engineering point of view [27]. However, fundamental investigation and understanding of the influence of lamination conditions on the electrode, especially catalyst, performance and the associated durability behavior have not been sufficiently addressed in the literature.

In this work, we systematically investigate catalyst layers treated by various hot-pressing conditions using electrochemical accelerated stress test (AST). We demonstrate that different lamination conditions being applied on the identical electrodes can cause different electrode interfaces. The resulting electrode structure has a direct impact on the electrode activity, platinum dissolution, platinum particle size and electrode surface element distribution when it is subjected to the electrochemical AST.

2. Experimental

The commercial catalyst HiSPEC® 9100 (Johnson Matthey), containing 57 wt% Pt supported on high surface area carbon black, was used to prepare the electrodes. The diameter of the platinum nanoparticles in this catalyst shows the largest fraction within 2–3 nm as confirmed before [28]. A catalyst ionomer electrode (CIE) microstructure containing about 30% Nafion ionomer (w/w) was prepared by coating of a catalyst/Nafion/water/alcohol suspension onto a gas diffusion layer (GDL), Sigracet® 35DC (SGL Group). The platinum loading was around 0.5 mg/cm^2 in the resulting CIE. Pieces of 2.5 cm by 2.5 cm were punched from the CIE and subjected to hot-pressing (lamination). The conditions were systematically varied based on the three parameters: pressure, temperature and duration, as shown in Table 1. Non-laminated electrode was used as control.

The electrodes were used as working electrode to perform cyclic voltammetry (CV) in a conventional three-electrode wet cell. A Radiometer® Hg/Hg_2SO_4 electrode was used as the reference electrode. All potential values are reported versus (vs.) the reversible hydrogen electrode (RHE). A glassy carbon rod was used as the counter electrode. The liquid electrolyte was 1 M H_2SO_4 (Sigma–Aldrich). The electrochemical AST was performed by potential cycling as a simulated start/stop test [29]. The AST was carried out between 0.4 and 1.6 V with a scan rate of 1 V/s. The CV evaluation was performed between 0 and 1.2 V, with a scan rate of 10 mV/s. The first cycle was abandoned, while the second cycle is reported in this work. Ar purging was maintained during the measurements with a constant flow of 0.2 mL/s. The experiments were carried out with an electrochemical workstation (Zahner® IM6). The connection between the sample and the device was established with a 0.2 mm thick gold wire.

The powder X-ray diffraction (XRD) pattern was collected by the use of a Panalytical X'Pert diffractometer. Data treatment was

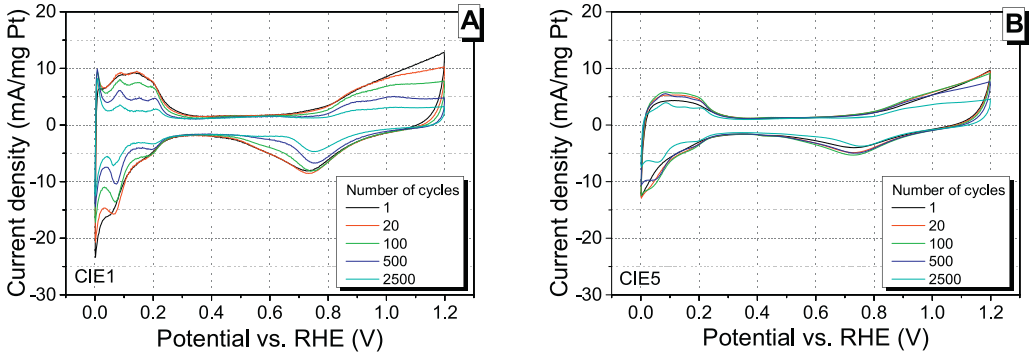

Fig. 2. Cyclic voltammograms of the electrode (A) CIE0 representing most electrodes studied in this work except CIE5, and (B) CIE5 under the electrochemical AST at ambient temperature.

assisted by X'Pert HighScope Plus. Dissolved platinum in the aqueous electrolyte was analyzed with a Varian® atomic absorption spectrotrometer (AAS) equipped with a graphite furnace providing high sensitivity. X-ray photoelectron spectroscopy (XPS) analysis was performed using a SPECS® system with Mg Kα (1253.6 eV) as the X-ray source. All binding energies were calibrated with respect to C 1s: C–C peak at 284.5 eV. The data was analyzed using CasaXPS™ and presented with Origin® Pro 9.1.

3. Results

3.1. Electrochemical performance

Typical cyclic voltammograms of the electrodes are shown in Fig. 2. The voltammograms from CIE0 in Fig. 2(A) represents most electrodes studied in this work except CIE5. Fig. 2(B) shows the evolution of CIE5.

In general, the catalyst in the electrode shows the characteristic platinum features of hydrogen adsorption and desorption at potentials between 0.05 and 0.4 V, platinum oxidation between 0.8 and 1.2 V during the positive sweep and oxide reduction between 1.0 and 0.5 V during the negative sweep. The platinum faces showed indistinct signals in the initial voltammograms. This is probably due to the surface of the catalyst being partially covered by the ionomer component and impurities, which may interfere with the proton adsorption/desorption. The degraded electrode showed clear platinum facets. This may be attributed to reduction of platinum oxide and/or re-deposition of the soluble platinum species (SPS). The columbic charge of the hydrogen adsorption was used to calculate the specific electrochemical surface area (specific ECSA) of the electrodes (based on the original catalyst loading). The resulting data are presented in Fig. 3.

Most electrodes (except the one laminated at 200 °C) follow similar trend and the difference is within 30%, as the case in Fig. 2(A). In the initial 20 cycles, the electrode performance reaches a maximum (where it is defined as 100% in the study). This is around 3–8% higher than the starting value. We interpret this as partial self-cleaning and partial ionomer reorganization to reach the most compatible surface configuration. After 2500 cycles, the specific ECSA decreases to between 34 and 42% of the max. specific ECSA. CIE5 was found to have a much lower initial specific ECSA than the rest of the electrodes (see also Fig. 2(B)). It took over 100 cycles to reach its maximum. Such performance is directly related to the hot-pressing temperature at 200 °C, which might partially damage the ionomer phase and destroy the tree-phase boundary. A detailed electrode performance in relation to the lamination conditions is shown in Fig. 4.

The initial specific ECSA (white bars) is seen to increase with the increasing lamination pressure, up to 7 bars, when other parameters were kept constant. A maximum specific ECSA was observed

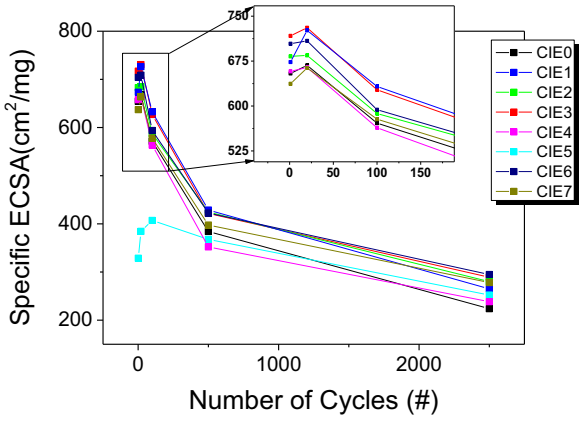

Fig. 3. Specific electrochemical surface area evolutions for the electrodes.

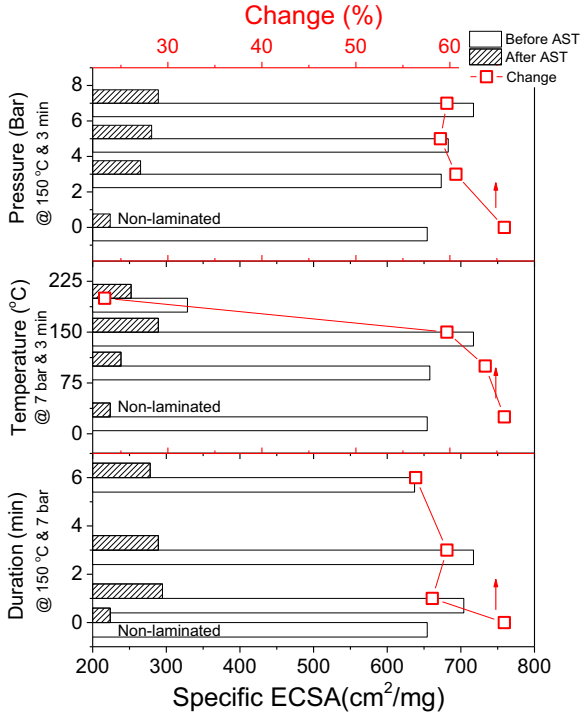

Fig. 4. Specific ECSAs of the electrodes prepared with various lamination conditions before and after the electrochemical AST.

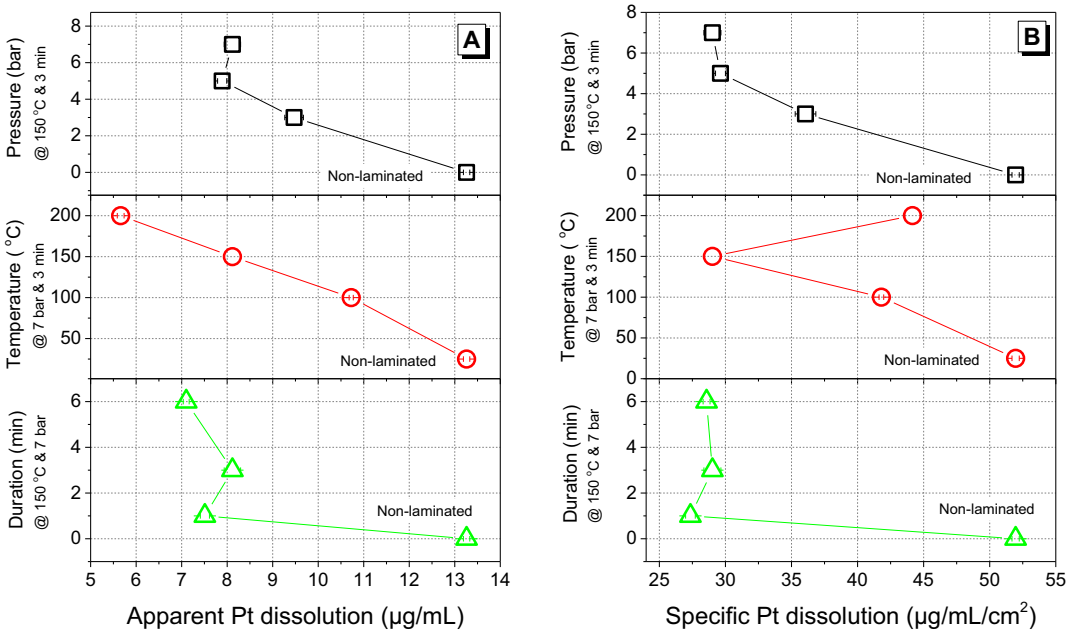

Fig. 5. Apparent (A) and specific (B) platinum dissolution of the electrodes prepared with various lamination conditions after the electrochemical AST.

for the electrode being laminated at 150 °C in comparison to other temperatures. A maximum specific ECSA was also observed for the electrode being laminated with 3 min in comparison to other durations. The degraded samples (striped bars) follow more or less the same trend. The relative percentage change (square symbols) between the initial and the end specific ECSA reflects the stability of the electrode.

3.2. Platinum dissolution

The acidic electrolyte used in the electrochemical AST was analyzed with atomic absorption spectroscopy. The apparent and specific (normalized to the ECSA) platinum dissolution behaviors of the various electrodes are shown in Fig. 5.

The platinum dissolution amount is directly related to the hot-pressing conditions. In Fig. 5(A), a reduction of the Pt dissolution was observed with an increase of the pressure up to 5 bars. Further increase of the pressure does not significantly affect the dissolution pattern. An almost linear reduction of the Pt dissolution amount is observed with an increase of the temperature up to 200 °C. The duration of the hot-pressing is not clearly related to the dissolution behavior of the catalyst. But a significant difference is noticed for the electrode with (1, 3 or 6 min) or without (0 min) the lamination step. In Fig. 5(B), the Pt dissolution is normalized to the ECSA in the electrode (in the unit of cm^2). A major difference is observed for the electrode hot pressed at 200 °C. This indicates that CIE5 has actually high Pt dissolution amount despite its low Pt accessibility.

3.3. XRD analysis

The various catalyst ionomer electrodes were studied with X-ray diffraction before and after the electrochemical AST. Typical diffraction patterns (similar for all 8 electrodes studied in this work) are shown in Fig. 6.

The diffraction peaks at around $2\theta = 39.6°$, 45.9°, 67.6°, 81.70° and 86.8° can be assigned to Pt (1 1 1), Pt (2 0 0), Pt (2 2 0), Pt (3 1 1) and Pt (2 2 2), respectively. Dominating peaks at approximate $2\theta = 26.6°$ and 54.7° are due to the diffraction in the highly graphitized carbon paper used in the GDL supporting the electrode. The peak at approximate $2\theta = 17.8°$ is due to the polymer contribution in the electrode structure. Pt crystallite size was evaluated from peak broadening of Pt (1 1 1) based on the Scherrer formula.

As we observed earlier [28], Nafion polymer has a diffraction peak at around $2\theta = 39.7°$, which coincidentally overlaps with platinum (1 1 1). The content of the ionomer in the electrode structure may have an influence on the peak width. Therefore, only relative changes are discussed. In general, the size of the platinum crystallites increases with the potential cycling. The relative diameter increment of the platinum nanoparticles after the 2500 electrochemical AST cycles is summarized in Fig. 7 in relation to the hot-pressing conditions.

The hot-pressing parameters also demonstrate a direct influence on the platinum particle size enlargement. The increment due to the AST is found to unilaterally decrease with the increase of the pressure within the test conditions. For lamination temperature and duration, a minimal diameter increment value was observed, at 150 °C and 3 min, respectively.

The hot-pressing conditions of temperature 200 °C and duration 6 min were found to be less effective in "keeping" the platinum in its shape. This may be caused by a partial damage of the polymer phase

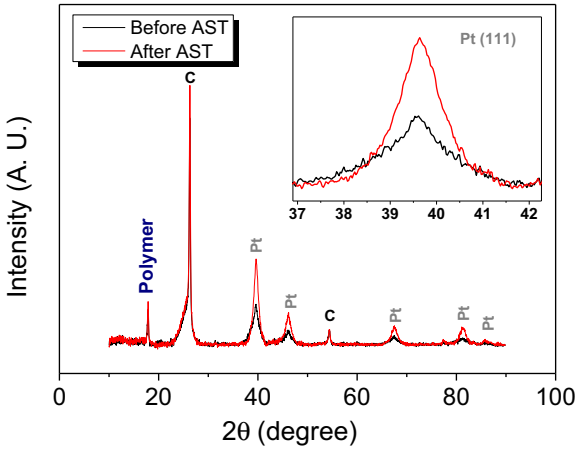

Fig. 6. XRD patterns of a catalyst ionomer electrode before and after the electrochemical AST.

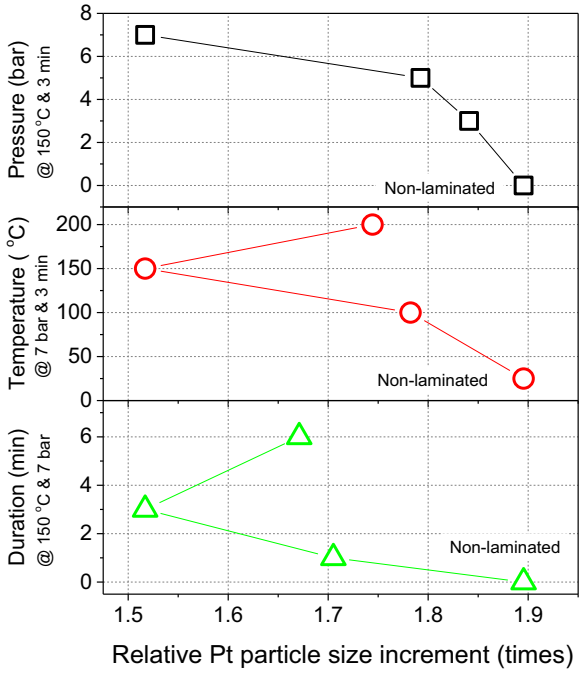

Fig. 7. Relative platinum nanoparticle diameter increment after the electrochemical AST as evaluated by XRD.

due to the excess heat during the electrode preparation (XPS also detects slight abnormality, see Section 3.4). Though bulk Nafion was reported to be stabile up to 300 °C [30,31] the ionomer thin film structure in the catalyst layer may be more vulnerable. Besides, the catalytic function of the platinum nanoparticles in the interface may lower the activation energy for the polymer degradation [31].

One of the important consequences of the platinum coalescence is the loss of active electrochemical surface area, and a reduction of the cell performance. Based on the platinum degradation mechanism [9]. (as mentioned before), a robust ionomer/interface structure can possibly lessen the platinum migration/agglomeration and carbon corrosion. These can reduce the enlargement of the platinum nanoparticles during the electrochemical operations. Moreover, crystallite migration and agglomeration is a potential-independent phenomenon [32]. A suitable ionomer structure may be beneficial not only under extreme conditions but also under normal cell operation circumstances.

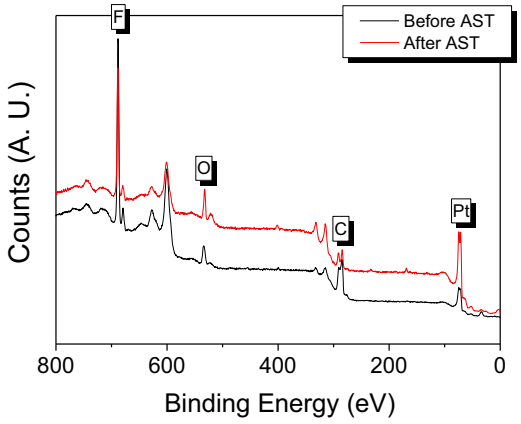

Fig. 8. XPS spectra before and after the electrochemical AST.

3.4. XPS surface analysis

X-ray photoelectron spectroscopy (XPS) was directly conducted on the catalyst ionomer electrodes without further treatment. Despite the 30 wt% ionomer loading in the electrode, no charging effect was experienced for any of the samples (both pristine and stressed) during the XPS experiment. The signal was collected according to an optimized condition developed earlier [33]. Typical XPS survey spectra (similar for all 8 electrodes studied in this work) before and after the electrochemical AST are shown in Fig. 8.

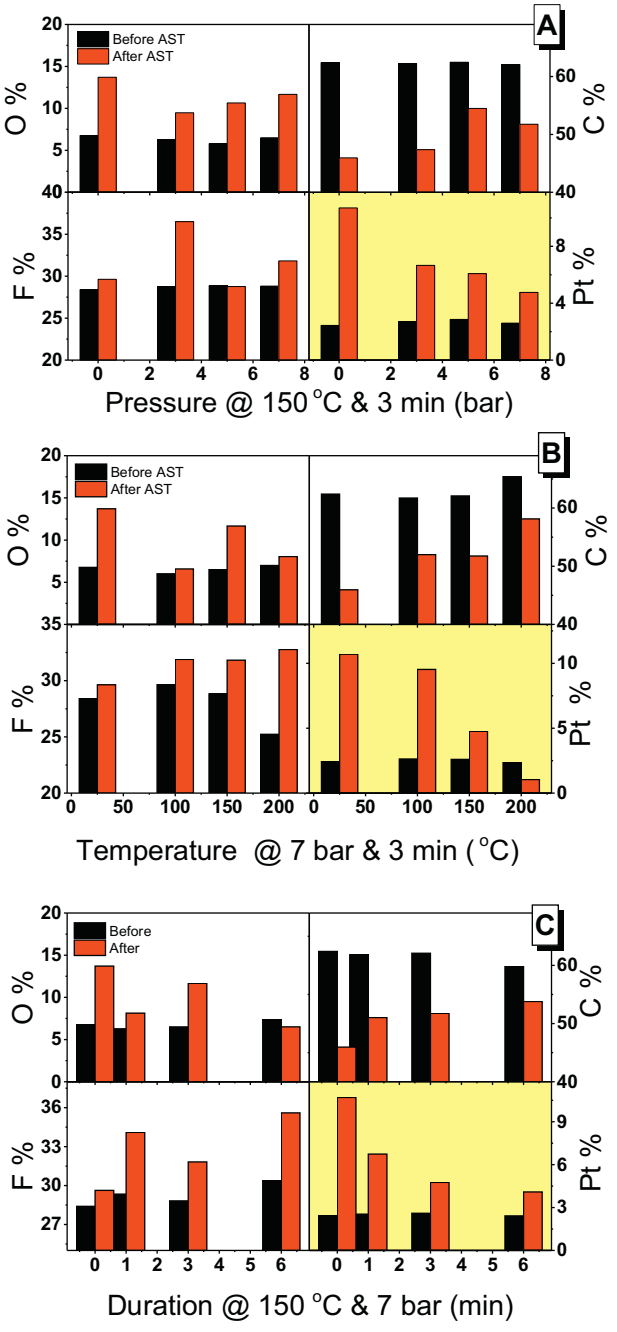

Fig. 9. Surface element composition in at % based on XPS for electrodes prepared at different hot-pressing conditions (A) pressure, (B) temperature and (C) duration before and after the electrochemical AST (the values at lowest pressure, temperature and duration are based on the non-laminated sample). (For interpretation of the references to color in the text, the reader is referred to the web version of this article.)

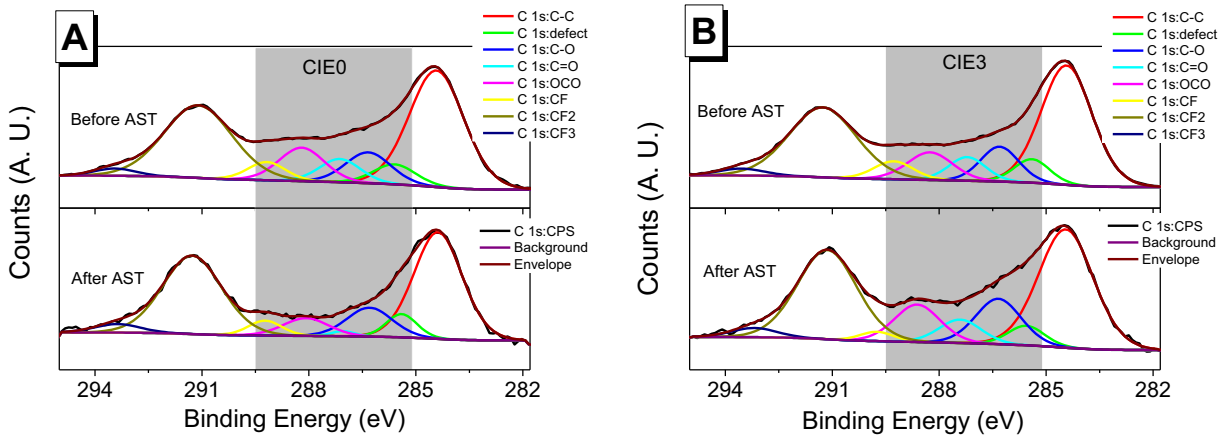

Fig.10. Deconvolution of C 1s high-resolution XPS spectra of CIE0 (A) and CIE3 (B).

The major surface elements are fluorine, carbon, oxygen and platinum. In relation to the hot-pressing conditions, the element contributions on the electrode surface before and after the AST were carefully studied and are summarized in Fig. 9.

The surface is dominated by carbon, which is attributed mainly to carbon support from the catalyst, but also slightly to the carbon content in the polymer. Fluorine is the second most abundant surface element. It is solely due to the ionomer contribution. Based on the repeated observation and detection volume, the detection of both carbon and fluorine indicates fairly homogeneous mixing of the two components, which are attractive toward each other, as reported before [34,35]. Oxygen is observed in all cases due to oxygen content in the ionomer and due to carbon and platinum oxides. Platinum was detected in various amounts.

The pristine surface chemical states (black bars) of the electrodes (except CIE5) are rather similar. This indicates that the various lamination conditions do not lead to a large difference on the top surface of the electrode. However, with the current procedure, XPS has no clue to the deeper interface information due to the small (1–2 nanometers) penetration depth of the technique, in comparison to the catalyst layer thickness of a couple of hundreds of micrometers [28]. Therefore, direct evidence of the electrode structure variation due to the hot-pressing conditions is not provided. This is among the subjects of our ongoing study. The surface of CIE5 shows that the fluorine content is lower and carbon and oxygen slightly higher than the other electrodes. This might indicate that the polymer was damaged during the lamination.

The surface chemical states of the electrochemically stressed electrodes (red bars) show significant difference from the pristine samples and with each other. In most cases, the platinum signal (i yellow windows in Fig. 9) was seen to increase significantly after the AST. This may be due to platinum migration and/or re-deposition of the SPS on the electrode surface during the electrochemical potential cycling. There is a clear trend that the increase of any of the lamination parameters (pressure, temperature or duration) decreases the platinum signal on the surface, indicating that this decreases the platinum degradation (redistribution to the surface). CIE5 showed less surface platinum after the AST. This might be due to depletion of the original surface Pt.

The carbon signal was seen to be significantly decreased after the AST (Fig. 8). This is mainly attributed to carbon corrosion and/or possible dissolution or degradation of the ionomer [36]. In most cases, the oxygen content increases significantly. This indicates carbon oxidation and/or polymer degradation [37] (due to the formation of peroxide or carbonyl groups from radical attack). The fluorine content increases, which might relate to the re-orientation or chemical structure change of the polymer.

Deconvolutions of the C 1s high resolution XPS spectra were specially studied. The representative spectra of CIE0 and CIE3 are shown in Fig. 10. The two dominating peaks appearing at binding energy (BE) around 284.5 and 291.2 eV are due to C–C (from the catalyst carbon support) and CF_2 (from the Nafion ionomer). Signal at BE around 295.6 eV is due to defective carbon bonding. Signals within BE region between 289.5 and 285.0 eV (high light as gray zone in the Fig. 10) are due to carbon oxides (e.g., CO, C=O, OCO). Signals at BE around 289.0 and 293.4 are due to CF and CF_3.

One of the obvious differences between the two electrodes toward the AST is that CIE3 shows significantly less change in the carbon oxides content (Fig. 10(B)) than that of CIE0 (Fig. 10(A)). The carbon oxides content in the electrodes laminated with other conditions (not shown here) were slightly more influenced by the AST of various degrees than that of CIE3, though they are more stable than that of CIE0.

4. Discussion

4.1. Electrode performance

Combining the various analyses, the electrode structure produced with the hot-pressing conditions at 7 bars, 150 °C and 3 min (CIE3) is the optimal electrode interface providing high catalyst utilization and high catalyst stability within the study. The catalyst in the non-laminated electrode (CIE0) shows lower performance than the laminated electrodes in general; though, exaggeration of the lamination condition may harm the ionomer phase, such as the case for CIE 5 and CIE7.

Broadly speaking, an increase of any of the parameters (pressure, temperature or duration) enhances the platinum durability within this study. However, this is a trade off with the initial performance. If the platinum is non-accessible at the beginning, the durability of the catalyst will be superb. This is the reason that CIE5 showed relatively small change in the specific ECSA after the accelerated stress test, since the catalyst may be covered with larger amount of contaminants and may not be “visible” in the electrode.

Moreover, due to the unique chemical structure, Nafion membrane is well known for its combination of crystalline and amorphous structure as demonstrated in crystallographic studies [38]. It has been shown [25]. that thermal treatment leads to the development of a more crystalline morphology. The high crystallinity restricted the absorption of water and led to a lower water content in the membrane. Consequently, the proton conductivity decreased. On the other hand, preparation of the MEA at a temperature below the glass transition temperature [25]. caused poor interfacial adhesion between the membrane and the electrode due

to poor polymer chain entanglement. So a balance needs to be reached.

The high specific ECSA of the electrode being laminated at the optimal conditions is due to its good interface structure. The commercial platinum catalyst with a platinum nanoparticle diameter of 2–3 nm is supported on a high surface area carbon black containing high porosity. Some of the catalyst nanoparticles trapped in the carbon pores are not connected to the proton phase. This will lower the specific ECSA. When the electrode is of optimized interface structure, the ionomer may penetrate into the pores and access the catalyst [39]. Moreover, when the optimized lamination is applied on the electrode, it also enhances the stability of the electrode. This is probably due to the compact structure and better protection of the individual components. Such electrode demonstrates high specific ECSA and stable performance.

4.2. Platinum dissolution and re-deposition

Based on the XPS studies, it is reasonable to assume that the surface properties of the platinum nanoparticles and the carbon support are rather similar in the eight investigated electrodes; in other words, the various hot-pressing conditions do not alter the Pt/C catalyst very much. Thus, the initial platinum dissolution abilities of the various electrodes might be assumed to be comparable. Hence, the significantly different dissolution amounts of the tested electrodes (Section 3.2) could probably be caused by the different efficiency in transport and/or re-deposition of the SPS within the electrode structure. Such efficiency can be related to instability of the catalyst, corrosion of the carbon support or any disruption of the electrode structure such as porosity, compactness, etc.

Another possibility for the different platinum dissolution behavior in the studied electrodes could be that the polymer may have different solubility for the SPS. This difference can easily be caused by the hot-pressing conditions [26] as well, since the hydrophilic domain, as the major transport path for the soluble species, maybe be modified due to re-orientation, crystallization of the polymer structure or possible damage of the sulfonate end groups.

4.3. Surface platinum enrichment

Notable surface platinum enrichment was observed in the study (Section 3.4). Such observation may be a consequence of carbon corrosion, ionomer degradation and/or platinum dissolution/re-deposition. However, a hydroquinone–quinone (HQ–Q) redox couple or thinning of the double layer capacity was hardly observed in the cyclic voltammograms of the catalyst ionomer electrodes (Section 3.1). This indicates that carbon corrosion is not severe.

The high carbon oxides content in the C 1 s spectrum at BE between 289.5 and 285.0 eV (Fig. 10, Section 3.4) may be due to the oxygen rich side chain (ether groups) in the Nafion ionomer, and possible interactions between the ionomer and the carbon support. The carbon oxides in a pristine electrode are around 60% relative to the C–C content. Though the carbon support may naturally contain oxides, their percentage is normally less than 15% relative to the C–C signal, as observed earlier [33]. In this sense, relative changes of the peaks (within BE between 289.5 and 285.0 eV) representing the functional groups may indicate robustness of the ionomer. The ionomer in the optimal electrode (CIE3) is more stable than that in the non-laminated electrode (CIE0) toward the AST. The enhanced stability may be due to increased crystallinity of the ionomer after the heat and pressure treatment. The ionomer stability of the laminated electrodes certainly contributes to reduce the enrichment of platinum on the surface. Moreover, a sound protonic path and a solid structure of the electrode are essential for a durable PEMFC.

Platinum dissolution/re-deposition or Ostwald ripening is one of the major degradation modes of the catalyst. A nearly linear

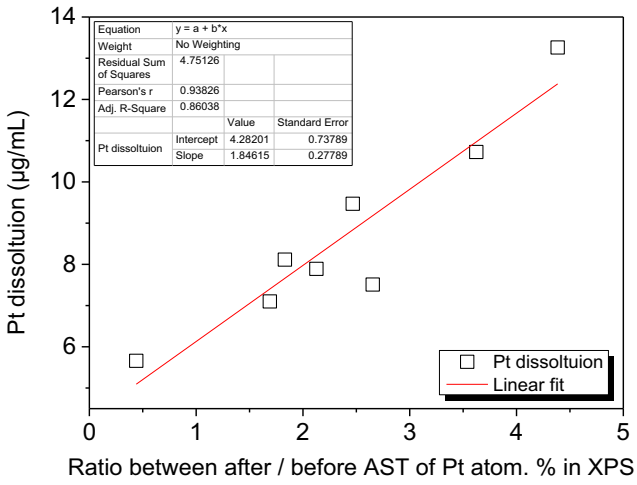

Fig. 11. Relation between platinum dissolution and platinum surface enrichment.

relationship was observed between the platinum dissolution amount in the electrolyte (Section 3.2) and the enrichment of the surface platinum (as reflected by the ratio between the XPS platinum atomic percentages after and before the AST), which is depicted in Fig. 11. Due to the large ion exchange capacity of the electrolyte, the SPS will primarily be present in the solution. However, the movement of the species for both dissolution and re-deposition may be affected by the coverage or solubility of the ionomer, which are directly affected by the electrode fabrication – lamination conditions. The ionomer crystallinity, the ionomer integrity and the associated properties of the SPS within the proton conducting phase are the major factors influencing on the platinum surface enrichment, or in general catalyst degradation and electrode stability.

4.4. Function of the ionomer

The primary function of the ionomer component in the electrode is, of course, to provide proton transport by expending the proton conducting phase three dimensionally. Another commonly accepted function of the ionomer is an electrode binder, which physically keeps electrode components as one entity. Moreover, the distribution and interaction between the ionomer and catalyst or catalyst support can lead to various electrode structures. Thus, another essential function of the ionomer in a composite electrode is construction of an interface. In this work we observed that interface optimization can be carried out through (but not only limited to) electrode hot-pressing. An optimal ionomer interface structure may play the following roles, as summarized in Fig. 12.

- Providing high platinum utilization: the ionomer may reach the catalysts tripped in the micropores which are not accessible to aqueous phase;
- Decreasing platinum migration and coalescence: the ionomer may act as a physical barrier preventing catalyst movement or merging;
- Reducing carbon corrosion triggered platinum detachment: the ionomer may cover the catalyst and carbon, which could protect them from oxidative reactions and separation from each other;
- Influencing transport property of the soluble platinum species (SPS) which may redeposit: the soluble amount and diffusivity of the SPS are closely related to the proton phase, which may have a great impact on the reaction kinetic of Pt dissolution and re-deposition.

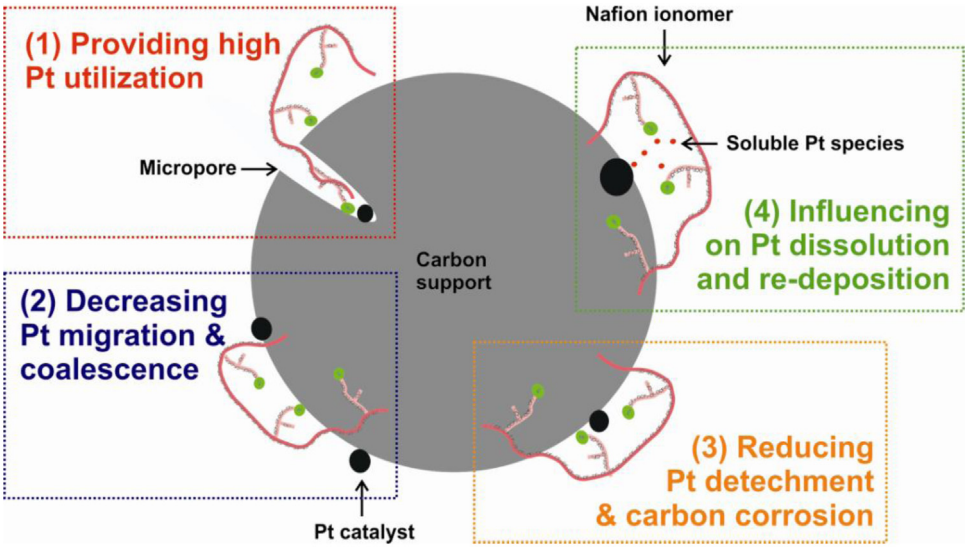

Fig. 12. Function of the ionomer in a catalyst ionomer electrode interface (not to scale).

5. Conclusions

Hot-pressing (lamination) conditions, comprising pressure, temperature and duration, applied on PEMFC electrodes were systematically studied. The electrode performance and durability were evaluated with respect to electrochemical surface area, Pt dissolution, Pt nanoparticle enlargement and electrode surface elements. In this study, the optimal hot-pressing conditions were found to be 7 bar, 150 °C and about 3 min. Carbon corrosion was found not to be severe. The property of the ionomer phase is a key factor in the preparation of an optimized and robust electrode structure. It can help to improve Pt visibility, decrease platinum migration and reduce carbon corrosion. Moreover, a robust interface structure can better maintain the three-phase boundary, reduce the platinum dissolution and assist in re-depositing dissolved platinum species as active electrocatalysts in the electrode. Development of the electrode interface can be of great benefit for the catalyst utilization, cell performance and durability.

Acknowledgements

The authors would like to give thanks for the financial support from the Danish PSO through the project DuraPEM III (2013-1-12064) and from the Danish Council for Strategic Research through the 4M Centre (12-132710).

References

[1] D. Zhao, J. Li, M.K. Song, B. Yi, H. Zhang, M. Liu, A durable alternative for proton-exchange membranes: sulfonated poly(benzoxazole thioether sulfone)s, Adv. Energy Mater. 1 (2011) 203–211.
[2] Y. Patil, S. Sambandam, V. Ramani, K. Mauritz, Perfluorinated polymer electrolytes hybridized with in situ grown titania quasi-networks, ACS Appl. Mater. Interfaces 5 (2013) 42–48.
[3] S. Park, Y. Shao, H. Wan, V.V. Viswanathan, S.A. Towne, P.C. Rieke, J. Liu, Y. Wang, Degradation of the ionic pathway in a PEM fuel cell cathode, J. Phys. Chem. C 115 (2011) 22633–22639.
[4] R. Uegaki, Y. Akiyama, S. Tojo, Y. Honda, S. Nishijima, Radical-induced degradation mechanism of perfluorinated polymer electrolyte membrane, J. Power Sources 196 (2011) 9856–9861.
[5] T. Nagai, H. Murata, Y. Morimoto, Influence of experimental conditions on the catalyst degradation in the durability test, J. Electrochem. Soc. 161 (2014) F789–F794.
[6] P. Pei, Q. Chang, T. Tang, A quick evaluating method for automotive fuel cell lifetime, Int. J. Hydrogen Energy 33 (2008) 3829–3836.
[7] S.S. Kocha, Polymer electrolyte membrane (PEM) fuel cells, automotive applications, in: Fuel Cells, Springer, 2013, pp. 473–518.
[8] A.J. Verhage, J.F. Coolegem, M.J. Mulder, M.H. Yildirim, F.A. de Bruijn, 30,000 h operation of a 70 kW stationary PEM fuel cell system using hydrogen from a chlorine factory, Int. J. Hydrogen Energy 38 (2013) 4714–4724.
[9] Y. Shao-Horn, W.C. Sheng, S. Chen, P.J. Ferreira, E.F. Holby, D. Morgan, Instability of supported platinum nanoparticles in low-temperature fuel cells, Top. Catal. 46 (2007) 285–305.
[10] Y. Zhou, K. Neyerlin, T.S. Olson, S. Pylypenko, J. Bult, H.N. Dinh, et al., Enhancement of Pt and Pt-alloy fuel cell catalyst activity and durability via nitrogen-modified carbon supports, Energy Environ. Sci. 3 (2010) 1437–1446.
[11] H. Oh, H. Kim, Efficient synthesis of Pt nanoparticles supported on hydrophobic graphitized carbon nanofibers for electrocatalysts using noncovalent functionalization, Adv. Funct. Mater. 21 (2011) 3954–3960.
[12] A.A. Kulikovsky, Understanding catalyst layer degradation in PEM fuel cell through polarization curve fitting, Electrocatalysis 5 (2014) 221–225.
[13] X. Zhao, W. Li, Y. Fu, A. Manthiram, Influence of ionomer content on the proton conduction and oxygen transport in the carbon-supported catalyst layers in DMFC, Int. J. Hydrogen Energy 37 (2012) 9845–9852.
[14] W. Li, M. Waje, Z. Chen, P. Larsen, Y. Yan, Platinum nanopaticles supported on stacked-cup carbon nanofibers as electrocatalysts for proton exchange membrane fuel cell, Carbon 48 (2010) 995–1003.
[15] L.A. Zook, J. Leddy, Density and solubility of Nafion: recast, annealed, and commercial films, Anal. Chem. 68 (1996) 3793–3796.
[16] B. Millington, S. Du, B.G. Pollet, The effect of materials on proton exchange membrane fuel cell electrode performance, J. Power Sources 196 (2011) 9013–9017.
[17] D. Henkensmeier, Q.K. Dang, N.N. Krishnan, J.H. Jang, H.J. Kim, S.W. Nama, T.H. Lima, Ortho-dichlorobenzene as a pore modifier for PEMFC catalyst electrodes and dense Nafion membranes with one porous surface, J. Mater. Chem. 22 (2012) 14602–14607.
[18] D. Fofana, S.K. Natarajan, J. Hamelin, P. Benard, Low platinum, high limiting current density of the PEMFC (proton exchange membrane fuel cell) based on multilayer cathode catalyst approach, Energy 64 (2014) 398–403.
[19] O.H. Kim, Y.H. Cho, S.H. Kang, H.Y. Park, M. Kim, J.W. Lim, D.Y. Chung, M.J. Lee1, H. Choe, Y.E. Sung, Ordered macroporous platinum electrode and enhanced mass transfer in fuel cells using inverse opal structure, Nat. Commun. 4 (2013) 2473.
[20] R.N. Bonifácioa, J.O.A. Paschoal, M. Linardi, R. Cuenca, Catalyst layer optimization by surface tension control during ink formulation of membrane electrode assemblies in proton exchange membrane fuel cell, J. Power Sources 196 (2011) 4680–4685.
[21] H.R. Brown, The adhesion between polymer, Annu. Rev. Mater. Sci. 21 (1991) 463–489.
[22] G. Fourche, An overview of the basic aspects of polymer adhesion. Part I: fundamentals, Polym. Eng. Sci. 35 (1995) 957–967.
[23] P.W. Majsztrik, A.B. Bocarsley, J.B. Benzinger, Viscoelastic response of nafion. Effects of temperature and hydration on tensile creep, Macromolecules 41 (2008) 9849–9862.
[24] K.A. Patankar, D.A. Dillard, S.W. Case, M.W. Ellis, Y. Li, Y.-H. Lai, M.K. Budinski, C.S. Gittleman, Characterizing fracture energy of proton exchange membranes using a knife slit test, J. Polym. Sci. B: Polym. Phys. 48 (2010) 333–343.
[25] H.Y. Jung, J.W. Kim, Role of the glass transition temperature of Nafion 117 membrane in the preparation of the membrane electrode assembly in a direct methanol fuel cell (DMFC), Int. J. Hydrogen Energy 37 (2012) 12580–12585.
[26] K. Froelich, H. Rauner, F. Scheiba, C. Roth, H. Ehrenberg, Welding of Nafion® – the influence of time, temperature and pressure, J. Power Sources 267 (2014) 260–268.

[27] O. Okur, C.L. Karada, F.J.B.E. San Okumus, G. Behmenyar, Optimization of parameters for hot-pressing manufacture of membrane electrode assembly for PEM (polymer electrolyte membrane fuel cells) fuel cell, Energy 57 (2013) 574–580.
[28] S.M. Andersen, E. Skou, Electrochemical performance and durability of carbon supported Pt catalyst in contact with aqueous and polymeric proton conductors, ACS Appl. Mater. Interfaces 19 (2014) 16565–16576.
[29] K.K. Tintula, A. Jalajakshi, A.K. Sahu, S. Pitchumani, P. Sridhar, A.K. Shukla, Durability of Pt/C and Pt/MC-PEDOT catalysts under simulated start–stop cycles in polymer electrolyte fuel cells, Fuel Cells 13 (2012) 158–166.
[30] S.M. Andersen, L. Grahl-Madsen, E. Skou, Studies on PEM fuel cell noble metal catalyst dissolution, Solid State Ionics 192 (2011) 602–606.
[31] H.J. Lee, M.K. Cho, Y.Y. Jo, K.S. Lee, H.J. Kim, E. Cho, et al., Application of TGA techniques to analyze the compositional and structural degradation of PEMFC MEAs, Polym. Degrad. Stab. 97 (2012) 1010–1016.
[32] L. Dubau, L. Castanheira, F. Maillard, M. Chatenet, O. Lottin, G. Maranzana, et al., A review of PEM fuel cell durability: materials degradation, local heterogeneities of aging and possible mitigation strategies, WIREs Energy Environ. 3 (2014) 540–560.
[33] S.M. Andersen, R. Dhiman, E. Skou, Chemistry of carbon polymer composite electrode – an X-ray photoelectron spectroscopy study, J. Power Sources 274 (2015) 1217–1223.
[34] S.M. Andersen, M. Borghei, R. Dhiman, H. Jiang, V. Ruiz, E. Kauppinen, E. Skou, Interaction of multi-walled carbon nanotubes with perfluorinated sulfonic acid ionomers and surface treatment studies, Carbon 71 (2014) 218–228.
[35] S.M. Andersen, M. Borghei, R. Dhiman, V. Ruiz, E. Kauppinen, E. Skou, Adsorption behavior of perfluorinated sulfonic acid ionomer on highly graphitized carbon nanofibers and their thermal stabilities, J. Phys. Chem. C 118 (2014) 10814–10823.
[36] T.C. Jao, G.B. Jung, S.C. Kuo, W.J. Tzeng, A. Su, Degradation mechanism study of PTFE/Nafion membrane in MEA utilizing an accelerated degradation technique, Int. J. Hydrogen Energy 37 (2012) 13623–13630.
[37] C. Chen, G. Levitin, D.W. Hess, T.F. Fuller, XPS Investigation of Nafion® membrane degradation, J. Power Sources, 169 169 (2007) 288–295.
[38] R.B. Moore, C.R. Martin, Chemical and morphological properties of solution-cast perfluorosulfonate ionomers, Macromolecules 21 (1988) 1334–1339.
[39] M. Uchida, Y.C. Park, K. Kakinuma, H. Yano, D.A. Tryk, T. Kamino, et al., Effect of the state of distribution of supported Pt nanoparticles on effective Pt utilization in polymer electrolyte fuel cells, Phys. Chem. Chem. Phys. 15 (2013) 11236–11247.